

Preparation of Cu- γ -Al₂O₃ Catalyst and Its Performance in Diphenylmethane Synthesis



This work is licensed under a Creative Commons Attribution 4.0 International License

N. Liangming,^a H. Jingbin,^a L. Dongmei,^{a,*} and H. Zhongdong^b

^aCollege of Petrochemical Technology, Liaoning Petrochemical University, Fushun, Liaoning, 113001, China

^bFushun Vocational Technology Institute, Fushun, Liaoning, 113122, China

doi: <https://doi.org/10.15255/CABEQ.2024.2375>

Original scientific paper
Received: October 17, 2024
Accepted: January 15, 2025

γ -Al₂O₃ has been widely studied as a very promising catalyst for the benzene alkylation reaction. In this study, the γ -Al₂O₃ support was prepared by the hydrothermal synthesis method, and the Cu- γ -Al₂O₃ catalyst was prepared by loading Cu through the impregnation treatment method with copper nitrate. Moreover, the Cu- γ -Al₂O₃ and γ -Al₂O₃ catalysts were characterized by X-ray diffraction (XRD), Fourier transform infrared spectroscopy (FT-IR), specific surface area measurement (BET), ammonia adsorption-desorption (NH₃-TPD), and pyridine infrared spectroscopy (Py-FTIR). The characterization results indicate that, compared with the γ -Al₂O₃ catalyst, the specific surface area, the pore volume and pore diameter of Cu- γ -Al₂O₃ become smaller, the total acid amount decreases, the amount of Lewis acid (L acid) increases, and the synergistic effect between Brønsted acid (B acid) and Lewis acid is enhanced. Meanwhile, the cases where the mass ratio of Cu- γ -Al₂O₃ was 3 %, 5 %, 10 %, and 15 % were investigated. Among these catalysts, the Cu- γ -Al₂O₃ with a mass ratio of 5% exhibited the highest performance in the benzene alkylation reaction. It is worth noting that compared with the previously reported Cu-Al-MCM-41, this catalyst showed a higher selectivity for diphenylmethane (94.8 % vs. 90.1 %).

Key words

benzyl alcohol, hydrothermal synthesis, Cu- γ -Al₂O₃, diphenylmethane, selectivity

Introduction

Diphenylmethane is widely used as a solvent in reactions, dyes, flame retardants, and as an intermediate in pharmaceutical synthesis^{1–5}. The most commonly used method for producing diphenylmethane currently is through the benzylation reaction of benzene with benzyl chloride under acidic conditions. However, this reaction produces hydrochloric acid, which can cause equipment corrosion and environmental pollution^{6–10}. The alkylation reaction of benzene and benzyl alcohol to synthesize diphenylmethane only produces water as a byproduct. However, the hydrogen on the benzene ring is not easily activated, resulting in a low yield of the product¹¹. Therefore, selecting a catalyst that can activate the hydrogen on the benzene ring and enhance the yield of the reaction between benzene and benzyl alcohol to synthesize diphenylmethane is highly significant. Currently, there is limited literature on the reaction between benzene and benzyl alcohol. However, Lu Meihuan and colleagues prepared a CuO-modified H-Y zeolite catalyst for this reaction, which demonstrated good activity during the catal-

ysis process, achieving a diphenylmethane yield of over 85 %¹². Our research group attempted to synthesize Cu- β -SBA-15 and Cu-Al-MCM-41 zeolites and applied them in the reaction of benzene with benzyl alcohol to synthesize diphenylmethane. The resulting Cu- β -SBA-15 zeolite catalyst showed some activity in the reaction, with water being the only byproduct; however, the yield of diphenylmethane synthesized was not as high as that reported in the literature^{13–18}. Research findings indicate that a larger surface area of the catalyst correlates with a higher number of active sites. However, a larger pore size is not necessarily better; excessively large pores can hinder effective collisions between reactants, negatively impacting the reaction performance. For the alkylation reaction of benzene and benzyl alcohol, having an excessive amount of strong acid in the catalyst is not necessarily beneficial. Instead, a moderate amount of medium-strength acid, along with the synergistic effect between strong and weak acids, can enhance both the selectivity and activity of the reaction. Therefore, our research group is summarizing our experiences and continuing to develop novel catalysts, with the aim of improving the yield of diphenylmethane from the reaction between benzene and benzyl alcohol.

*Corresponding author: Liu Dongmei (email: ldmwain1234@126.com)

γ -Al₂O₃ exhibits excellent thermal stability and can maintain good catalytic activity under high temperature and pressure conditions^{19,20}. Additionally, γ -Al₂O₃ has a highly crystalline hexagonal phase structure, which provides high activity. It typically exists as nano-sized particles, offering excellent dispersion that exposes more active sites on the catalyst surface to the external environment. This characteristic allows hydroxyl and oxygen atoms to better adsorb the hydrogen on the benzene ring, thereby enhancing the catalytic activity^{21,22}. Moreover, γ -Al₂O₃ possesses a mesoporous structure that provides an optimal pore channel configuration for the reactants, increasing the diffusion rate of the reactants and thereby enhancing the reaction rate²³. γ -Al₂O₃ also possesses certain acid-base properties, allowing it to function as an acidic catalyst in proton transfer reactions and as a basic catalyst in electron transfer reactions²⁴. This dual functionality enhances the interactions between benzene and benzyl alcohol, improving the selectivity of the reaction.

Noble metals are typically used as co-catalysts due to their partially filled d-electron orbitals, which facilitate the adsorption of reactants with moderate strength. This characteristic is beneficial for the formation of intermediate active compounds, significantly accelerating the rate of chemical reactions²⁵. In recent years, the prices of noble metals have remained high, prompting efforts to seek non-noble metals to enhance catalyst performance due to cost considerations. Copper is a promising non-noble metal^{26–28}. Wang²⁹ and colleagues successfully prepared a series of copper-promoted layered silicate nanotube (CuPSNT) catalysts, which were applied to the chemical synthesis of cyclohexane through the phenol HDO reaction. This work demonstrates that copper plays a key role in the phenol HDO process. Loading metal copper onto γ -Al₂O₃ provides Cu ions with high chemical affinity, enabling them to form coordination bonds with the oxygen on the catalyst surface. These coordination bonds facilitate the adsorption and activation of reactant molecules on the catalyst surface, thereby improving catalytic efficiency³⁰. Therefore, this experiment prepared the Cu- γ -Al₂O₃ catalyst, aiming to enhance the conversion rate and selectivity of the reaction between benzene and benzyl alcohol. The results from the synthesis of diphenylmethane through the reaction between benzene and benzyl alcohol will be used to identify the optimal conditions for the preparation of the Cu- γ -Al₂O₃ catalyst.

Experimental

Materials

The main reagents used in this experiment were: Ammonia water (NH₃·H₂O, 28 wt%); Aluminum sulfate octadecahydrate (Al₂(SO₄)₃·18H₂O;

99.5 %); Ammonium bicarbonate (NH₄HCO₃; 99 %); Barium chloride (BaCl₂; 99 %); Copper nitrate (Cu(NO₃)₂·3H₂O; 99 %); Benzene (C₆H₆; 99.5 %); Benzyl alcohol (C₇H₈O; 99 %), which were all purchased from Shanghai Macklin Biochemical Co., Ltd. Deionized water (H₂O) was self-made in the laboratory.

Sample characterizations

X-ray diffraction (XRD)

The XRD experiment was carried out using a Rigaku D/max-RB diffractometer (Japan) to measure the diffraction patterns. CuK α radiation was employed, and a graphite curved crystal monochromator was placed in front of the scintillation counter. The tube voltage was 40 kV, tube current was 100 mA, radius of the goniometer was 185 mm, and the diaphragm system was set at DS = SS = 1 mm and RS = 0.15 mm. Each sample was filled into a glass sample holder to a depth of 0.5 mm, and the surface was compacted with smooth flat glass. The continuous scanning mode of θ -2 θ was adopted, with a step length of 0.02 mm and a scanning speed of 4 mm(2 θ)° min⁻¹.

Fourier transform infrared spectroscopy (FT-IR)

Infrared analysis was conducted using a Spectrum GX Fourier transform infrared spectrometer (Perkin-Elmer, USA) with the KBr pellet method. The spectral resolution was 4 cm⁻¹, the measurement range was 4000 – 400 cm⁻¹, the scanning signals were accumulated 16 times, the OPD speed was 0.2 cm s⁻¹, and the gain was 1.

N₂ adsorption-desorption (BET)

The ASAP-2010 nitrogen adsorption analyzer (Micromeritics, USA) was used for the adsorption-desorption analysis. During this process, 0.15 g of the sample was placed into a quartz tube and kept at 300 °C under a pressure of less than 1.3 Pa for 360 minutes to remove moisture. The isothermal adsorption curve can be used to calculate the specific surface area, total pore volume, and pore size distribution. The specific surface area was calculated by the Brunauer-Emmett-Teller (BET) formula, and the total pore volume and pore size distribution were obtained from the desorption curve of the isotherm using the DFT method.

Ammonia temperature-programmed desorption (NH₃-TPD)

This analysis was performed on a TP-5000-II adsorption analyzer (Tianjin Xianquan Instrument Co., Ltd.). The flow rate of the carrier gas N₂ was 40 mL min⁻¹. The temperature was increased from

120 °C to 600 °C at a rate of 10 °C min⁻¹. After being kept at a constant temperature of 600 °C for 30 minutes, it was decreased to 120 °C and kept constant. After adsorbing NH₃ for 30 minutes, it was purged with N₂ for 2 hours, and then the temperature was increased to 600 °C at a rate of 10 °C min⁻¹.

Pyridine infrared spectroscopy (Py-FTIR)

The Py-FTIR analysis was performed using a Cary660 infrared spectrometer produced by (Agilent Technologies, USA) combined with a self-developed oil-free glass vacuum adsorption in-situ infrared characterization system, designed by the Dalian Institute of Chemical Physics.

X-ray photoelectron spectroscopy (XPS)

X-ray photoelectron spectroscopy was employed to qualitatively and quantitatively analyze the elemental composition on the surface of materials, atomic valence states, and the energy state distribution by analyzing the electron binding energy. In this study, a K-Alpha X-ray photoelectron spectrometer (Thermo Fisher Scientific) was used with the following test parameters: a monochromatic Al K α light source with an energy of 1486.6 eV, and an acceleration voltage of 15 kV.

Sample preparation

Preparation of γ -Al₂O₃ molecular sieve

To prepare γ -Al₂O₃, 44 g of Al₂(SO₄)₃·18H₂O and 30 g of NH₄HCO₃ were weighed and dissolved separately to form two solutions. At 75 °C, both solutions were simultaneously added at a flow rate of 4 mL min⁻¹ into a three-neck flask maintained at 75 °C with continuous stirring. The pH of the system was adjusted to alkaline using ammonia water. After the reaction was completed, the system temperature was adjusted down to 70 °C and left to age for 1 h. Vacuum filtration was then performed, and the solid was washed with deionized water until no SO₄²⁻ was detected using BaCl₂. The washed sample was oven-dried at 110 °C for 12 hours, yielding the γ -Al₂O₃ precursor, designated as A1.

A1 was dispersed in a 1.25 mol L⁻¹ NH₄HCO₃ solution and stirred thoroughly. The mixture was aged at 70 °C for 2 h. After aging, the precipitate was filtered and washed until neutral. The washed sample was oven-dried at 110 °C for 12 hours, and then calcined at 450 °C for 5 h in a muffle furnace, producing A2.

A2 was subsequently dispersed in a 1.25 mol L⁻¹ NH₄HCO₃ solution, stirred at a controlled rate for 1.5 h at 50 °C, and then aged at 70 °C for 1 h. After aging, the precipitate was filtered and washed

until neutral. The washed sample was oven-dried at 110 °C for 12 hours and calcined for 5 h at 600 °C in a muffle furnace to obtain γ -Al₂O₃.

Preparation of Cu- γ -Al₂O₃ catalyst

The incipient wetness impregnation method was used to prepare a catalyst with a mass ratio of Cu to γ -Al₂O₃ of 1:20. Based on the desired Cu loading, an appropriate amount of Cu(NO₃)₃ was weighed and dissolved in a sufficient quantity of deionized water to form a solution. At room temperature, γ -Al₂O₃ was added to the solution and stirred thoroughly to mix. The mixture was allowed to stand at room temperature for 12 h. It was then oven-dried at 110 °C for 12 hours and calcined at 600 °C for 5 h in a muffle furnace. The resulting sample was labeled as Cu- γ -Al₂O₃.

Catalyst performance tests

The catalytic activity of the catalyst was evaluated in a microreactor with an inner diameter of 10 mm. A total of 3.0 grams of catalyst, corresponding to a volume of 6 mL, was loaded into the reactor. All the experimental data for the evaluation of the catalyst performance were obtained under the following reaction conditions: reaction temperature of 110 °C, mass ratio of benzene to benzyl alcohol of 1:4, and the reactants were pumped continuously into a fixed-bed reactor for continuous reaction at a mass hourly space velocity of 1.5 h⁻¹, with nitrogen introduced as the carrier gas to maintain the reaction pressure at 1 MPa. After the reaction, the products underwent two-stage condensation and cooling. The outlet products were analyzed using an HP4890 gas chromatograph. The chromatographic detection conditions were as follows: an OV-101 polar chromatographic column with a specification of 0.25 mm \times 50 m and a hydrogen flame ionization detector were used. The vaporization temperature was 200 °C, the detector temperature was 280 °C, and the initial temperature was 40 °C. Temperature programming was employed. Nitrogen served as the carrier gas, and the area normalization method was applied to calculate the conversion rate (X) of benzyl alcohol, the selectivity (S) of diphenylmethane, and the yield (Y) of diphenylmethane. The calculation formulas are as follows:

$$X = \frac{W_0 - W_t}{W_0} \cdot 100 \% \quad (1)$$

$$S = \frac{W'_t}{W_0 - W_t} \cdot 100 \% \quad (2)$$

$$Y = \frac{W'_t}{W_0} \cdot 100 \% \quad (3)$$

where W_0 is the molar mass of benzyl alcohol in the reactant; W_t is the molar mass of benzyl alcohol after reaction, and W_t' is the molar mass of benzyl alcohol consumed to synthesize diphenylmethane.

Results and discussion

Influence of Cu- γ -Al₂O₃ preparation conditions on the reaction of diphenylmethane synthesis

Effect of γ -Al₂O₃ prepared at different pH levels on diphenylmethane synthesis

At an aging time of 1 h at a temperature of 70 °C, and a roasting time of 5 h at a temperature of 600 °C, the effects of γ -Al₂O₃ prepared at different PH values on the synthesis of diphenylmethane from benzene and benzyl alcohol were investigated. The results are shown in Fig. 1(a). As seen in Fig. 1(a), increasing the pH value from 7.5 to 8.5, enhanced the yield of diphenylmethane from 30.5 % to 36.04 %. This was because, when the benzyl alcohol molecules diffused onto the surface of γ -Al₂O₃, the interaction between the opposite charges generated an electrostatic attraction at the basic sites, forming hydrogen bonds^{31,32}. Additionally, the γ -Al₂O₃ surface contained basic sites, such as Al-OH or Al-O⁻, which could accept H⁺, further facilitating the formation of stable hydrogen bonds. These hydrogen bonds enhanced the adsorption capacity of benzyl alcohol molecules on the catalyst surface, increasing their reactivity. As a result, the hydroxyl groups in the benzyl alcohol molecules became more active and more likely to participate in the reaction³³, leading to the production of diphenylmethane and other products³⁴. However, when the pH value exceeded 8.5, the conversion rate and selectivity of the reaction decreased. This was because, at relatively high pH values, γ -Al₂O₃ exhibits stronger basicity. At this point, the concentration of hydroxide ions on the catalyst surface increased, promoting the hydroxyl alkylation reaction of benzene molecules to form benzoic acid and benzyl alcohol. Therefore, the optimal pH for γ -Al₂O₃ is 8.5, and the yield of diphenylmethane is 36.04 %.

Effect of aging time of γ -Al₂O₃ catalysts on diphenylmethane synthesis

The effects of γ -Al₂O₃ aging time on diphenylmethane synthesis was investigated at a roasting time of 5 h, aging temperature of 70 °C, roasting temperature of 600 °C, and pH of 8.5. The results are shown in Fig. 1(b). As seen in Fig. 1(b), increasing the aging time from 0.5 h to 1 h, increased the yield of diphenylmethane on γ -Al₂O₃ from 28.3 % to 36.04 %. However, beyond 1 h, the conversion and selectivity of the reaction began to decline. This

was because grains of an appropriate size provided more surface active sites, increasing the contact area between reactants and active sites, thereby improving catalytic efficiency³⁵. However, with prolonged aging, the grain boundary length of adjacent grains exceeded the critical value due to grain growth, leading to an enhanced grain boundary blocking effect³⁶, restricting contact between reactants and active sites, thereby reducing catalytic activity. Therefore, the optimal aging time of γ -Al₂O₃ is 1 h, with a diphenylmethane yield of 36.04 %.

Effect of aging temperature of γ -Al₂O₃ on diphenylmethane synthesis

The effects of γ -Al₂O₃ aging temperature on diphenylmethane synthesis were investigated at a roasting time of 5 h, aging time of 1 h, a roasting temperature 600 °C, and pH 8.5. The results are shown in Fig. 1(c).

As seen in Fig. 1(c), increasing the aging temperature from 60 °C to 70 °C, improved the diphenylmethane yield from 28.5 % to 36.04 %. However, at the aging temperature of 75 °C, the conversion and selectivity of the reaction began to decline. This was because, during the aging process of γ -Al₂O₃, increased temperature promoted the growth of grain and expanded the lattice defects³⁷, which served as active sites for adsorption of reactant molecules³⁸. However, as the aging temperature increased further, oxygen molecules adsorbed to the oxygen vacancies, reducing the number of active sites on the catalyst surface³⁹, thereby reducing the catalytic performance of γ -Al₂O₃. Therefore, the optimal aging temperature is 70 °C, with a yield of diphenylmethane of 36.04 %.

Effect of copper loading on γ -Al₂O₃ on diphenylmethane synthesis

The effects of $m_{Cu}:m_{\gamma-Al_2O_3} = 3\%$, 5 %, 10 %, and 15 % on the synthesis of diphenylmethane were investigated at a roasting time of 5 h, aging time of 1 h, roasting temperature of 600 °C, pH of 8.5, and aging temperature of 70 °C. The reaction results are shown in Fig. 1(d). As shown in Fig. 1(d), both the conversion rate and selectivity of Cu- γ -Al₂O₃ is higher than those of Cu(3 %)- γ -Al₂O₃ after γ -Al₂O₃ was loaded with Cu. This was because an appropriate loading of copper provided more active sites, enhancing interactions between reactant molecules and the catalyst, thereby increasing reaction activity⁴⁰. However, with higher copper loadings, both the conversion rate and selectivity of the reaction decreased due to the aggregation or accumulation of metal particles, which reduced the effective surface area and catalyst activity⁴¹. Therefore, an optimal copper loading enhanced the activity of γ -Al₂O₃ and

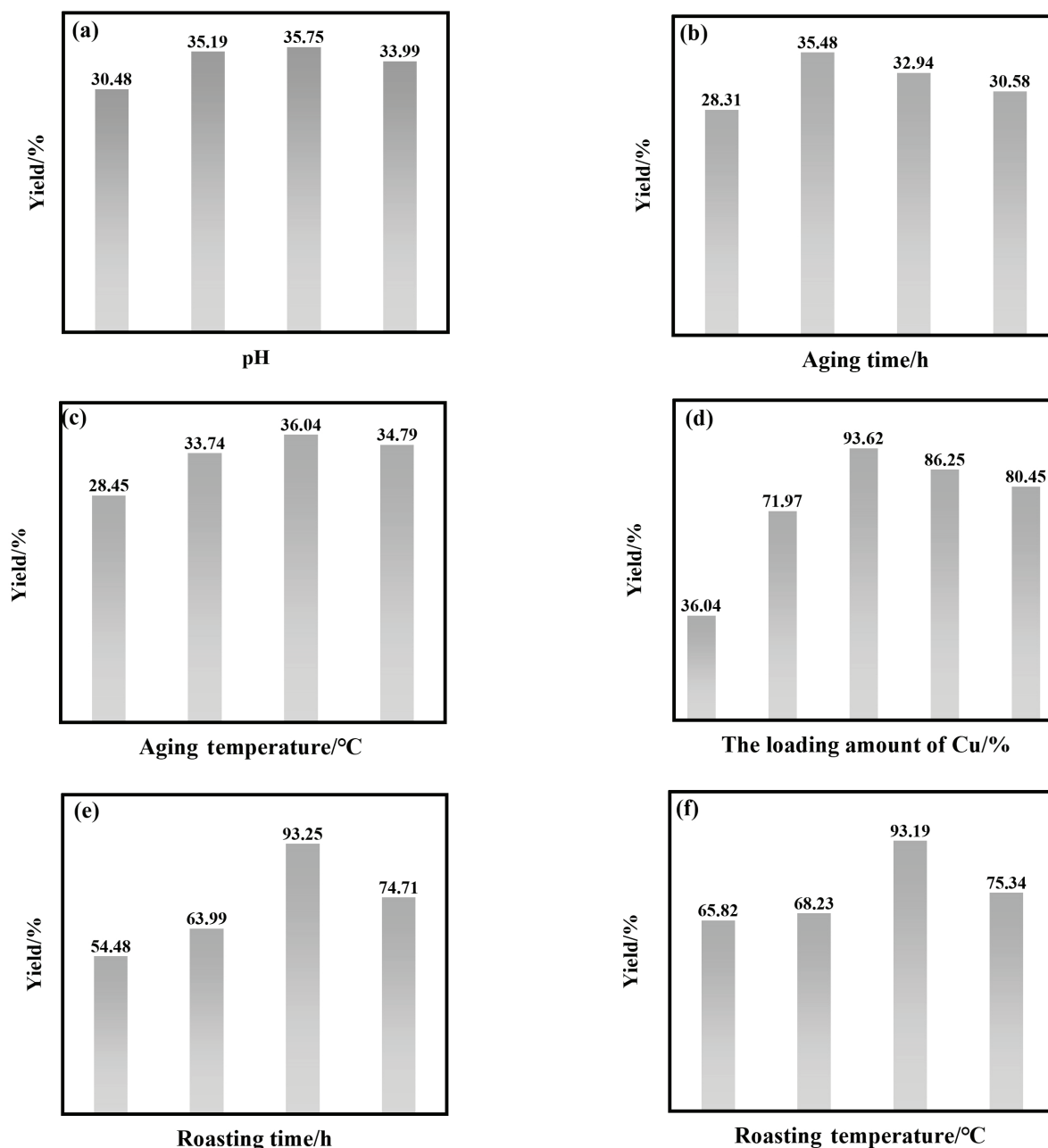


Fig. 1– Effect of catalyst preparation conditions on the synthesis of diphenylmethane

improved the selectivity for the desired product. As shown in Fig. 1(d), with the ratio of $m_{\text{Cu}}:m_{\gamma\text{-Al}_2\text{O}_3}$ of 5 %, the Cu- γ -Al₂O₃ catalyst demonstrated the best performance in synthesizing diphenylmethane.

Effect of roasting time of Cu- γ -Al₂O₃ catalyst on diphenylmethane synthesis

The influence of the Cu- γ -Al₂O₃ catalysts synthesized under different roasting times on the synthesis reaction of diphenylmethane was investigated at the aging time of 1 h, roasting temperature of 600 °C, pH value of 8.5, aging temperature of 70 °C, and mass ratio of $m_{\text{Cu}}:m_{\gamma\text{-Al}_2\text{O}_3}$ of 5 %. The results are shown in Fig. 1(e).

As shown in Fig. 1(e), extending the roasting time of the Cu- γ -Al₂O₃ catalyst from 4 h to 5 h increased the yield of diphenylmethane from 54.5 % to 94.03 %. However, further extending the roasting time to 5.5 h resulted in a decrease in yield to 74.7 %. This trend can be attributed to the influence of roasting time on Cu- γ -Al₂O₃ catalyst particle size⁴². Suitable particle size exhibits better diffusion and transport properties while reducing inter-particle interactions, thereby improving the surface activity of the catalyst⁴³. Additionally, the appropriate roasting time can induce surface restructuring of the catalyst, during which some Cu ions or oxygen atoms may rearrange and form new structures, creating

more active sites on the catalyst surface⁴⁴. However, when the roasting time exceeded 5 h, the Cu- γ -Al₂O₃ particles increased in size leading to extended diffusion pathways and mass transfer limitations, thereby reducing the catalytic efficiency⁴⁵, and the yield of diphenylmethane. Thus, a roasting time of 5 h provided the most favorable reaction conditions for the Cu- γ -Al₂O₃ catalyst to achieve the best performance for the reaction between benzene and benzyl alcohol, resulting in the highest diphenylmethane yield of 94.03 %.

Effect of roasting temperature of Cu- γ -Al₂O₃ catalyst on diphenylmethane synthesis

The effect of roasting temperature on diphenylmethane synthesis was investigated under the following conditions: aging time of 1 h, pH 8.5, aging temperature of 70 °C, $m_{\text{Cu}}:m_{\gamma\text{-Al}_2\text{O}_3}$ of 5 %, and a roasting time of 5 h. The results are shown in Fig. 1(f).

As shown in Fig. 1(f), increasing the calcination temperature of Cu- γ -Al₂O₃ catalyst from 550 °C to 600 °C improved the yield of diphenylmethane, reaching 93.2 %. However, further increasing the calcination temperature to 650 °C reduced the yield of diphenylmethane to 75.3 %. This was because at calcination temperatures below 600 °C, the crystal structure remains underdeveloped, which negatively affects the reactant adsorption and catalytic performance. Incomplete calcination at low temperatures prevents the proper formation of pore structures, restricting reactant access to the active sites and thereby reducing catalytic activity. Moreover, inadequate decomposition of catalyst precursors can result in fewer active centers, thus resulting in lower catalyst activity. At an optimal calcination temperature, the grain growth and elimination of grain boundaries are promoted, thereby increasing the surface area of the catalyst. A larger surface area allows for the adsorption of reactants and enhances the catalytic reactions, thus improving catalytic performance⁴⁶. Additionally, calcining at a suitable temperature may result in smaller and uniformly distributed Cu particles on the support⁴⁷. Smaller particle sizes contribute to a higher exposure of Cu on the catalyst surface, further boosting the reaction activity. When the roasting temperature exceeds 600 °C, roasting accelerates grain growth, leading to a decrease in surface area and a reduction in the number of available active sites on the catalyst, ultimately lowering its activity⁴⁸. Therefore, the Cu- γ -Al₂O₃ catalyst exhibited the best catalytic activity at a calcination temperature of 600 °C.

The findings of this study provide theoretical support and information references for the industrial production of diphenylmethane from benzene and benzyl alcohol. Table 1 lists the types of catalysts

Table 1 – *Properties of different catalysts used in diphenylmethane synthesis*

Sample	Conversion rate/%	Selectivity/%	Yield/%	References
CBV20A	45.9	16.3	7.48	36
FAPO4-5	69.5	98.8	29.67	37
AlSBA-15(45)	99.99	76.79	54.87	38
5Mo-FeP-NT	59	93	54.87	39
Fe-ZSM-5	95.2	85.23	81.13	40
H β	33.3	89.1	29.67	41

used for the synthesis of diphenylmethane from benzene and benzyl alcohol in recent years along with their catalytic performances, and compares them with the present work. Obviously, Cu- γ -Al₂O₃ showed better performance.

Based on the experimental analysis, the optimal reaction conditions for the Cu- γ -Al₂O₃ catalyst in the reaction between benzene and benzyl alcohol were as follows: γ -Al₂O₃ aging time of 1 h, aging temperature of 70 °C, pH of 8.5, and Cu to γ -Al₂O₃ ratio of 5 %. The roasting temperature for Cu- γ -Al₂O₃ was 600 °C, and the roasting time was 5 h. Under these conditions, the Cu- γ -Al₂O₃ catalyst exhibited the best performance, achieving a reaction conversion rate of 99.2 %, selectivity of 94.0 %, and a diphenylmethane yield of 94.03 %. The following sections present the characterization analysis of the synthesized γ -Al₂O₃ and the Cu- γ -Al₂O₃ catalyst under these conditions.

Catalyst characterization

XRD analysis

Fig. 2 presents the XRD patterns of the γ -Al₂O₃ and Cu- γ -Al₂O₃ samples. Before and after loading Cu on γ -Al₂O₃, the diffraction peaks corresponding to the (311), (222) and (400) crystal planes appear at $2\theta = 38^\circ$, 46° and 67° , respectively, which are consistent with literature reports⁵⁵. This indicates that the synthesized support was a pure phase, and the γ -Al₂O₃ crystal phase possessed high purity and cleanliness. Additionally, the crystal structure of γ -Al₂O₃ did not undergo significant changes before and after Cu loading. The slightly lower intensity of the characteristic peaks after Cu loading compared to γ -Al₂O₃ is likely due to some degree of lattice distortion caused by the interaction between Cu²⁺ and the γ -Al₂O₃ surface. The decrease in the intensity of the (311) diffraction peak for Cu- γ -Al₂O₃ and the reduction in lattice parameters are related to lattice distortion⁵⁶. The absence of characteristic Cu peaks in the XRD pattern indicates that CuO was highly dispersed on the γ -Al₂O₃ surface.

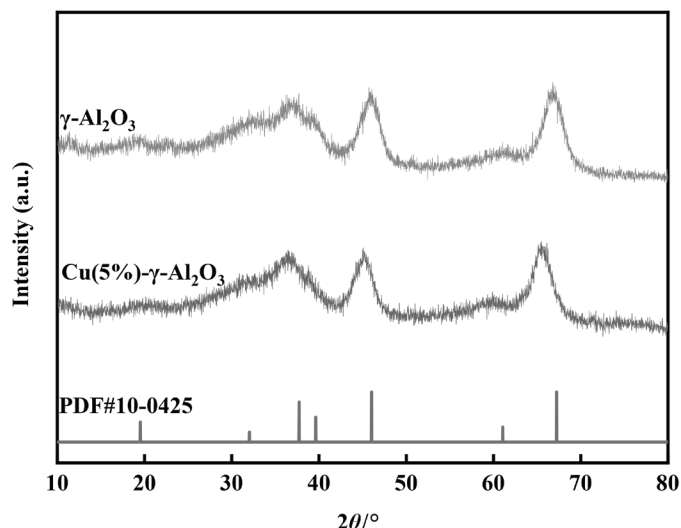
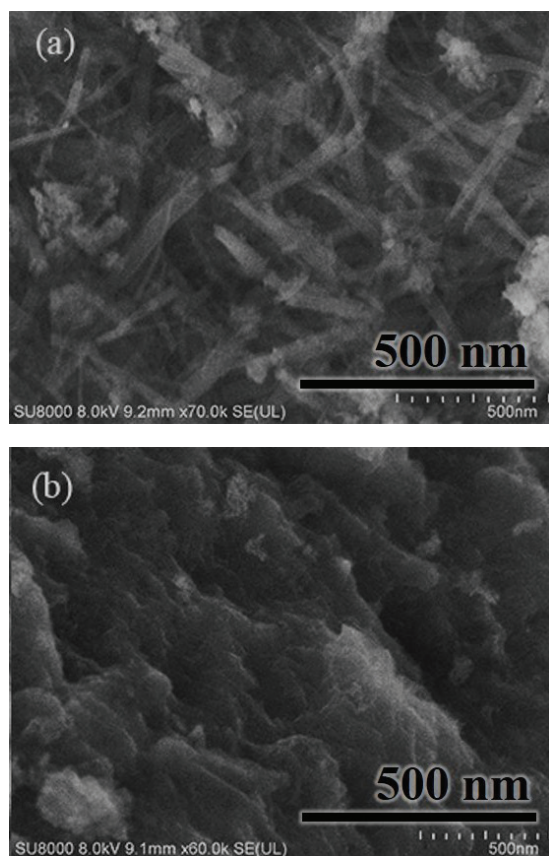


Fig. 2 – XRD spectra of the catalyst

Fig. 3 – SEM images of the catalysts (a) γ -Al₂O₃; (b) Cu (5 %)- γ -Al₂O₃

SEM analysis

Fig. 3 presents the SEM images of γ -Al₂O₃ and Cu- γ -Al₂O₃. Fig. 3(a) shows that γ -Al₂O₃ consists of uniform nanoscale rod-shaped crystals with consistent morphology and uniform dimensions. Fig. 3(b) shows that the Cu- γ -Al₂O₃ particles were larger and possessed relatively loose structure. The Cu- γ -Al₂O₃

sample, prepared via the equal-volume impregnation method, exhibited good dispersion without significant agglomeration.

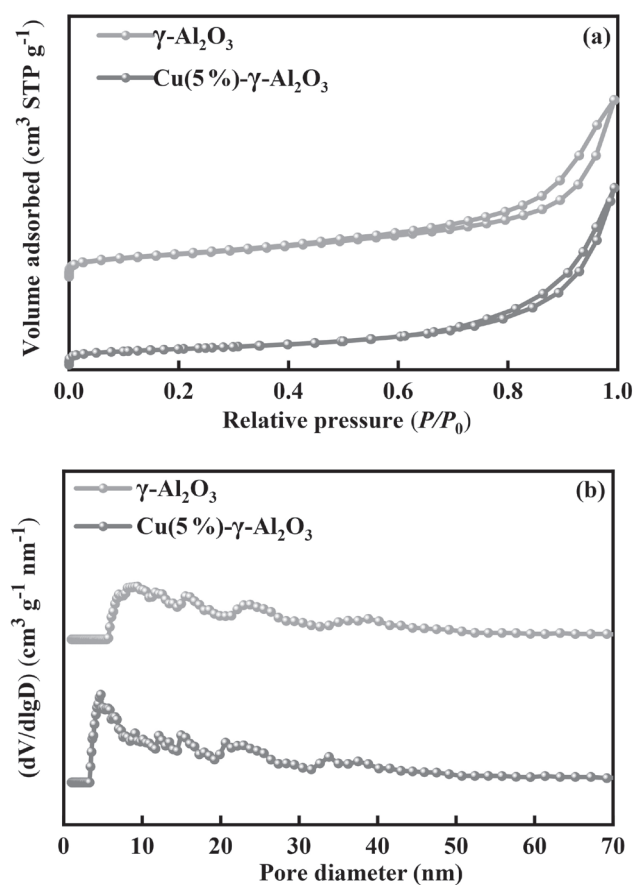
N₂ adsorption-desorption analysis

Fig. 4 shows the N₂ adsorption-desorption isotherms and DFT pore size distribution curves of γ -Al₂O₃ and Cu- γ -Al₂O₃ catalysts, while Table 2 presents the textural properties of γ -Al₂O₃ before and after Cu loading.

According to IUPAC classification, the N₂ adsorption-desorption isotherms of both samples were of type IV⁵⁷. The N₂ adsorption amount of each sample increased gradually at relative pressures below 0.6, indicating the presence of microporous structures in the catalysts. In the relative pressure range of 0.6 to 1.0, the adsorption amount increased rapidly, suggesting the presence of mesoporous

Table 2 – Textural properties of the catalyst

Sample	$S/(m^2 g^{-1})$	$V/(cm^3 g^{-1})$	D/nm
γ -Al ₂ O ₃	536.05	0.88	7.42
Cu(5 %)- γ -Al ₂ O ₃	487.96	0.71	4.32

Fig. 4 – N₂ adsorption-desorption isotherms and DFT pore size distribution curves of γ -Al₂O₃ and Cu- γ -Al₂O₃ catalysts

structure with larger pore sizes in the samples⁵⁸. γ -Al₂O₃ exhibited an H1-type hysteresis loop at $P/P_0 = 0.6$. After Cu loading, the hysteresis loop appeared at $P/P_0 = 0.7$. This shift occurred because, during the Cu loading process, the Cu particles blocked the pores, reducing the number of accessible pores for nitrogen adsorption. Consequently, the hysteresis loop for Cu- γ -Al₂O₃ shifted to a higher relative pressure⁵⁹.

From Fig. 4 and Table 2, it can be observed that the pore size distribution mainly falls between 4 and 45 nm, with a relatively larger number of mesopores in the 4 to 20 nm range. Fig. 4 and Table 2 also show that the specific surface area, pore volume, and pore size of γ -Al₂O₃ decrease after Cu loading. This is because the Cu loading occupies part of the pore space leading to a reduction in pore size⁶⁰. Although the pore size of Cu- γ -Al₂O₃ catalyst was smaller than that of γ -Al₂O₃, the molecular diameter of benzol was approximately 0.96 nm. Smaller pore sizes can better restrict the diffusion rate of reactant molecules and increase the local concentration of reactant molecules, thereby enhancing the effective collision frequency of reactants on the catalyst⁶¹. This allows the reactants to be adsorbed better onto the active sites of the catalyst. After Cu loading with, the specific surface area and pore volume of the catalyst decreased, but the density of the active sites on the catalyst increased. This enhanced the adsorption of reactants on the catalyst surface, thereby improving the mass transfer rate of the catalyst⁶².

NH₃-TPD analysis

Fig. 5(a) shows the NH₃-TPD characterization of Cu- γ -Al₂O₃ and γ -Al₂O₃, while Table 3 outlines the acid properties of both samples. As seen in Fig. 5(a), each sample exhibited an NH₃ desorption peak between 150~200 °C and 400~450 °C, corresponding to the weak acid centers and strong acid centers,

Table 3 – Acid properties of the catalysts

Sample	γ -Al ₂ O ₃	Cu(5 %)- γ -Al ₂ O ₃
L	0.375	0.401
150 °C	B	0.002
	L/B	187.5
	L	0.046
450 °C	B	0.001
	L/B	46
Weak acid quantity/mmol g ⁻¹	1.103	1.166
Strong acid content/mmol g ⁻¹	1.710	1.625
Total acid content/ mmol g ⁻¹	2.813	2.791

respectively. A further comparison of the data in Table 3 indicated that, although the total acid amount of the catalyst slightly decreased with the introduction of Cu, the types of acid centers on the catalyst surface remained unchanged⁶³. This might be due to

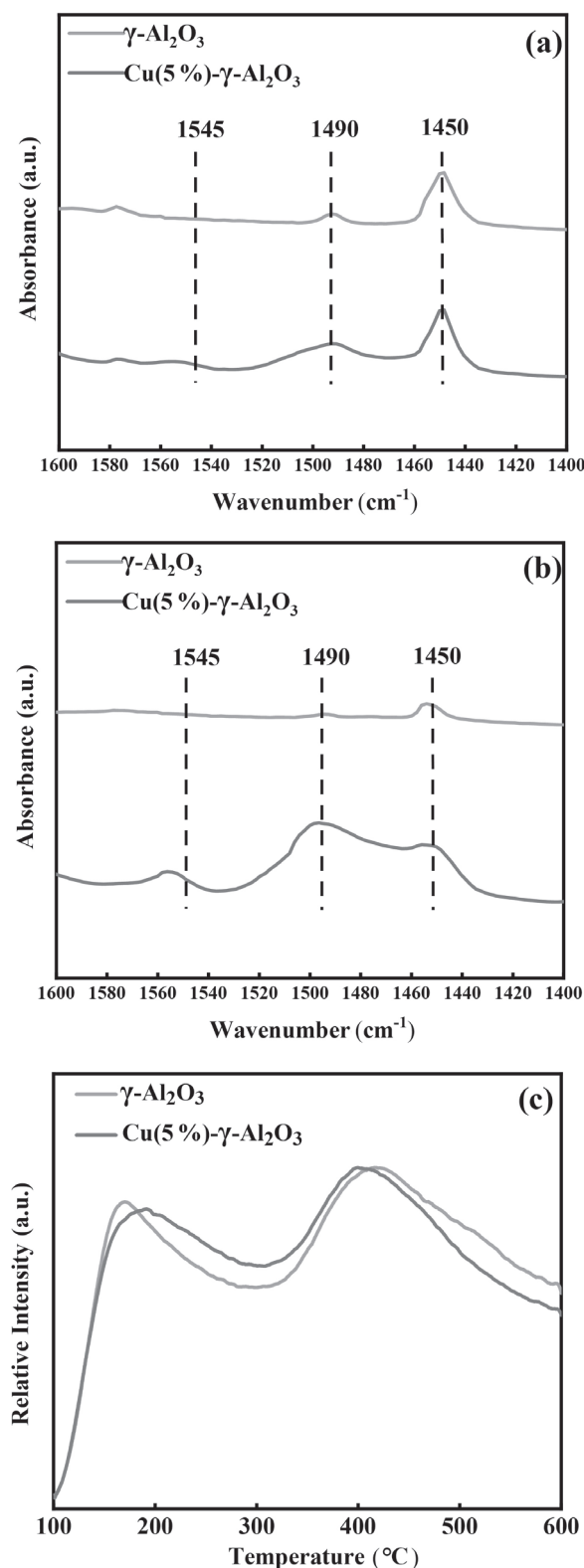


Fig. 5 – Py-FTIR pattern of γ -Al₂O₃ and Cu(5 %)- γ -Al₂O₃: (a) 150 °C, (b) 400 °C, (c) NH₃-TPD pattern of catalysts

the interaction between the active sites on the surface of Cu particles and the surface hydroxyl groups of γ -Al₂O₃ during the loading process⁶⁴, resulting in partial charge transfer to the hydroxyl groups. Consequently, some acid sites lose their activity, leading to a reduction in the overall acid amount. As seen from Table 3, the addition of Cu altered the surface acidity and the distribution of acid sites on the catalyst.

Py-FTIR analysis

Fig. 5(a) shows the Py-FTIR characterization of the two molecular sieves Al-MCM-41 and Cu(5 %)-Al-MCM-41, while Table 3 presents the acidity distribution parameters of the two molecular sieves. In Fig. 5(b) and Fig. 5(c), the peak at 1450 cm⁻¹ corresponds to the L-acid sites, the peak at 1545 cm⁻¹ corresponds to the B-acid sites, and the peak at 1490 cm⁻¹ corresponds to the B+L acid sites⁶⁵. By comparing the total acid distribution at 160 °C with the strong acid distribution at higher temperatures, it can be observed that, compared to Al-MCM-41, the Cu(5 %)-Al-MCM-41 molecular sieve shows an increase in both the peak intensity and peak area of the absorption peak at 1450 cm⁻¹, which corresponds to the L-acid sites. The peak area represents the amount of acid, indicating an increase in the L-acid amount in the catalyst. However, the absorption peak intensity and peak area at 1545 cm⁻¹, corresponding to the B-acid sites decrease, indicates a reduction in the B-acid amount. Moreover, the reduction in the amount of B-acid is less than the increase in the amount of L-acid. This can be observed in the change in the peak area at the absorption peak position of 1490 cm⁻¹, indicating that the addition of copper increased L-acid sites while reducing B-acid sites. This change in the L/B ratio led to improved selectivity and diphenylmethane yield, and enhanced the catalytic activity. This suggests that the more L-acid sites present in the molecular sieve, the more favorable the catalytic reaction for the production of diphenylmethane, corroborating the reaction mechanism.

FT-IR analysis

Fig. 6(a) shows the infrared spectra of γ -Al₂O₃ and Cu- γ -Al₂O₃. Both samples exhibited absorption peaks at 3480 cm⁻¹, attributed to the stretching vibration of -OH. This indicates that both samples contained surface hydroxyl groups⁶⁶. The absorption peaks between 500–1800 cm⁻¹ for γ -Al₂O₃ before and after Cu loading show minimal variation, indicating that the surface properties of the samples remained unchanged after Cu loading. Among these, the absorption peaks at 1629 cm⁻¹ and 1514 cm⁻¹ are attributed to the bending vibration of the

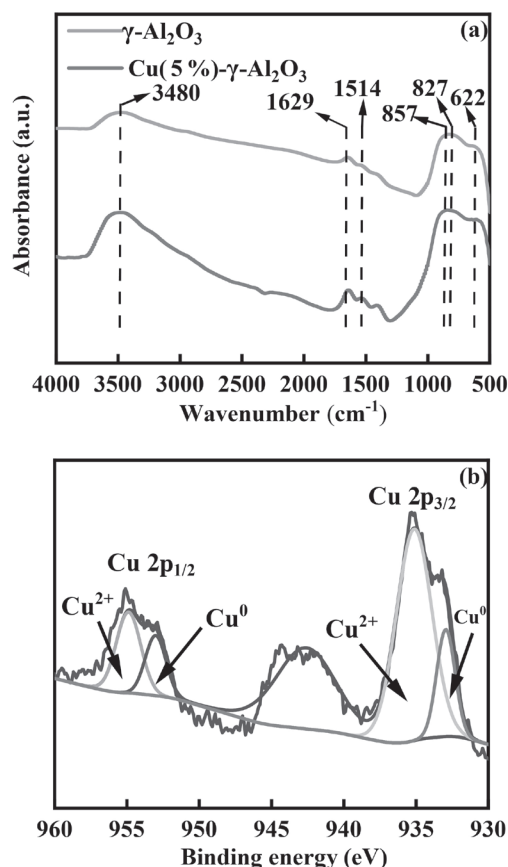


Fig. 6 – (a) FT-IR spectra of the catalyst; (b) XPS spectra of surface elements of Cu- γ -Al₂O₃

-OH group in water⁶⁷. The absorption peaks at 857 cm⁻¹ and 622 cm⁻¹ in both samples correspond to the asymmetric stretching vibration of Al-O-Al and Al-O within the aluminum-oxygen cluster. For Cu- γ -Al₂O₃, the peak at 857 cm⁻¹ shifted to a higher wavenumber compared to γ -Al₂O₃ and the characteristic peak changed from a sharp peak to a broad peak. This was because the introduction of Cu particles interacted with the Al-O or Al-OH bonds in γ -Al₂O₃, leading to the formation of stronger chemical bonds between the metal and these oxygen or hydroxyl groups. Consequently, the characteristic peak broadened and the corresponding vibration frequency shifted to a higher wavenumber⁶⁸. Thus, this peak was attributed to the lattice vibration peak of copper oxide. The FT-IR characterization of the catalyst further confirmed that the synthesized samples were γ -Al₂O₃ and Cu- γ -Al₂O₃.

XPS analysis of two molecular sieves

The elemental composition of the surface of the Cu (5 %)- γ -Al₂O₃ catalytic material were analyzed using XPS with Gaussian fitting, and the results are shown in Fig. 6(b). This spectrum includes two main peaks, Cu 2p_{1/2} and Cu 2p_{3/2}, as well as one satellite peak. Through peak deconvolution, the

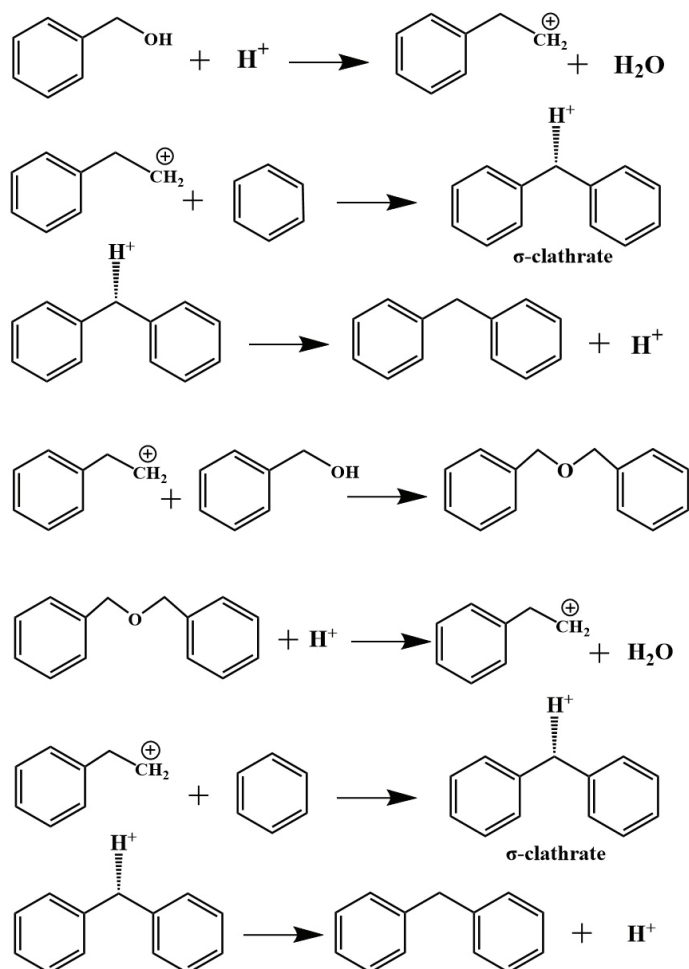


Fig. 7 – Catalytic reaction mechanism for the synthesis of diphenylmethane from benzene and benzyl alcohol

two main peaks can be further divided into components corresponding to Cu^{2+} and Cu^0 . Cu^{2+} is generally Lewis acid, capable of accepting electron pairs and activating the benzene ring, which is beneficial for electrophilic substitution. The high reducing ability of Cu^0 can provide electrons to the σ -complex, facilitating its transformation into diphenylmethane, thereby improving the selectivity of the reaction⁶⁹. The synergistic effect of Cu^{2+} and Cu^0 endows the catalyst with enhanced catalytic performance and selectivity, which is consistent with the pyridine infrared results.

Benylation reaction mechanism of benzene with benzyl alcohol

Based on experimental findings, a plausible mechanism for benzene alkylation by Cu (5 %)- γ -Al₂O₃ is proposed, as presented in Fig. 7. The alkylation reaction of benzene with benzyl alcohol follows the carbocation mechanism⁷⁰. The electron pair trans-

fers between the benzyl alcohol and the Lewis acid sites on the catalysts to form benzyl carbocation ($PhCH_2^+$). Then, the electrophilic carbocation attacks the benzene ring adsorbed on the active site of catalyst to form a σ -complex⁷¹. Finally, the σ -complex regains stability by releasing H^+ , resulting in the formation of diphenylmethane. Simultaneously, the benzyl carbocation can react with another benzyl alcohol to produce dibenzyl ether (DBE). The ether bond on DBE has strong electronegativity due to the unpaired electrons of oxygen atom, so the C–O bond of DBE could be polarized when absorbed to Lewis acid sites of catalyst with subsequent benzyl carbocation formation. An electron pair from the benzene ring subsequently attacks $PhCH_2^+$ to produce diphenylmethane⁷². In this study, Cu- γ -Al₂O₃ played multiple crucial roles in the entire mechanism process. Its acidic sites provided the necessary chemical environment for the polarization of the benzene ring and the stabilization of the carbocation intermediate, promoting the directional progress of the reaction. Meanwhile, the Cu^{2+} sites participated in the activation process of the alkylating reagent. Through the interaction with the reactant molecules, they changed the electron cloud structure and reactivity of the reactants, and cooperated with the acidic sites to jointly promote the smooth progress of the benzylation carbocation mechanism, thereby improving the reactivity and selectivity of the reaction.

Conclusion

γ -Al₂O₃ and Cu- γ -Al₂O₃ were synthesized via the hydrothermal and impregnation methods. The effects of γ -Al₂O₃ preparation conditions and copper loading on the yield of diphenylmethane were investigated. The obtained materials were characterized using XRD, SEM, BET, NH₃-TPD, XPS, Py-FTIR, and FT-IR techniques. Characteristics such as crystal structure, particle morphology, pore structure, acid sites, and chemical bonding before and after Cu loading, the promoting effect of Lewis acid sites, and the synergistic effect of Cu^{2+} and Cu^0 , were demonstrated. The catalytic performance of γ -Al₂O₃ and Cu- γ -Al₂O₃ was evaluated using the synthesis of diphenylmethane from benzene and benzyl alcohol as a reaction probe. Cu- γ -Al₂O₃ achieved the best diphenylmethane yield. It is worth noting that, compared to the previously reported Cu-Al-MCM-41, the Cu- γ -Al₂O₃ catalyst exhibited higher efficiency (94.03 % vs. 90.1 %), primarily due to its stronger acidity.

ACKNOWLEDGEMENTS

The National Natural Science Foundation of China (21978125) funded the project.

CONFLICT OF INTEREST

The authors declare no conflict of interest.

DATA AVAILABILITY STATEMENT

The data that support the findings of this study are available from the corresponding author upon reasonable request.

Reference

- Juan, S. M., Kristof, D. W., Marius, W. E., Stian, S., Ton, V. W. J., Veronique, V. S., Pablo, B., Unni, O., Benzene co-reaction with methanol and dimethyl ether over zeolite and zeotype catalysts: Evidence of parallel reaction paths to toluene and diphenylmethane, *J. Catal.* **349** (2017) 136. doi: <https://doi.org/10.1016/j.jcat.2017.03.007>
- Lu, M. H., Gudala, S., Liu, Z., Sharma, A., Liu, X. Y., Yang, J. X., Catalytic benzylation of arenes using metal-ion modified HY zeolites for sustainable synthesis, *Cailiao Huaxue Wuli* **328** (2024) 130034. doi: <https://doi.org/10.1016/j.matchemphys.2024.130034>
- Zhang, Q., Feng, Z. F., Niu, Y. L., Chen, D. M., Yao, N., Zhang, P., Tang, Y. L., Du, J. B., The molecular structure and spectra of diphenylmethane under the external electric field, *Chem. Physics Letters* **849** (2024) 141419. doi: <https://doi.org/10.1016/j.cplett.2024.141419>
- Zhou, C. H., Luo, X. P., Ge, Z. H., Li, X. N., Cai, Y., Guo, H. Q., Hydrogen production from sodium borohydride by ZnCl₂ treated defatted spent coffee ground catalyst, *Inter. Hydrogen. J.* **45** (2020) 9733. doi: <https://doi.org/10.1016/j.ijhydene.2020.01.244>
- Yin, D. H., Li, C. Z., Tao, L., Ning, Y. Y., Shan, H., Du, L. Y., Synthesis of diphenylmethane derivatives in Lewis acidic ionic liquids, *J. Mol. Catal. A: Chem.* **245** (2006) 260. doi: <https://doi.org/10.1016/j.molcata.2005.10.010>
- Hu, X. C., Chuah, G. K., Stephan, J., Room temperature synthesis of diphenylmethane over MCM-41 supported AlCl₃ and other Lewis acids, *Appl. Catal. A* **217** (2001) 1. doi: [https://doi.org/10.1016/S0926-860X\(01\)00574-9](https://doi.org/10.1016/S0926-860X(01)00574-9)
- Divya S. Nair, Manju, K., Highly selective synthesis of diphenyl methane via liquid phase benzylation of benzene over cobalt doped zinc nanoferrite catalysts at mild conditions, *J. Saudi Chem. Soc.* **23** (2019) 127. doi: <https://doi.org/10.1016/j.jscs.2018.05.011>
- Ren, F. F., Ma, J. H., Li, R. F., Study on benzylation of aromatics based on multistage porous zeolite catalyst, *Taiyuan Ligong Daxue Xuebao* **48** (2017) 317. doi: <https://doi.org/10.16355/j.cnki.issn1007-9432tyut.2017.03.007>
- Isamu, S., Masahiko, S., The catalytic Friedel-Crafts alkylation reaction of aromatic compounds with benzyl or allyl silyl ethers using Cl₂Si(OTf)₂ or Hf(OTf)₄, *Tetrahedron Lett.* **43** (2002) 6391. doi: [https://doi.org/10.1016/S0040-4039\(02\)01376-X](https://doi.org/10.1016/S0040-4039(02)01376-X)
- Maryam, F., Reza, M. B., Toubia, H., Synthesis promotion and product distribution for HZSM-5 and modified Zn/HZSM-5 catalysts for MTG process, *Fuel* **120** (2016) 248. doi: <https://doi.org/10.1016/j.fuel.2016.04.120>
- Hou, S. X., Xie, W. L., Vantomme, A., Cheetham, A. K., Su, B. L., Three-dimensional hierarchical meso/macroporous Mo/Ce/TiO₂ composites enhances biodiesel production from acidic soybean oil by transesterification-esterifications, *Energy Con Man.* **305** (2024) 118273. doi: <https://doi.org/10.1016/j.enconman.2024.118273>
- Bokhimi, X., Sánchez, V. J., Pedraza, F., Crystallization of sol-gel boehmite via hydrothermal annealing, *J. Solid State Chem.* **166** (2002) 182. doi: <https://doi.org/10.1006/jssc.2002.9579>
- Han, J. B., Ning, L. M., Wang, L., Liu, D. M., Zhang, Q. K., Feng, K. X., Preparation of Cu- β -SBA-15 molecular sieve catalyst and its effect on the synthesis of diphenylmethane from benzene and benzyl alcohol, *Yingyong Huagong* **52** (2023) 675. doi: <https://doi.org/10.16581/j.cnki.issn1671-3206.2023.03.002>
- Li, X., Fang, C., Huang, L., Yu, J., Enhanced carbon dioxide adsorption and carrier separation over amine functionalized zirconium metal organic framework/gold/indium oxide for boosting photocatalytic carbon dioxide reduction. *J. Colloid Interface Sci.* **655** (2024) 485. doi: <https://doi.org/10.1016/j.jcis.2023.11.028>
- Lu, Z. M., Zhang, Q. J., Chen, R. Y., Yu, D. Q., A new diphenylmethane derivative from *Uvaria kuriz* with cardiovascular activity, *Chinese Journal of Natural Medicines* **9** (2011) 90. doi: <https://doi.org/10.3724/SP.J.1009.2011.00090>
- Hou, Z. H., Yokuhara, T., Catalytic synthesis of diphenylmethane from benzene and formalin with water-to-lerant solid acids, *Applied Catalysis A: General* **216** (2001) 147. doi: [https://doi.org/10.1016/S0926-860X\(01\)00546-4](https://doi.org/10.1016/S0926-860X(01)00546-4)
- Preethi, L. E. M., Sivakumar, T., Palanichami, M., Room temperature efficacious synthesis of diphenylmethane over Fe/Al-MCM-41 catalysts, *Catal. Commun.* **11** (2010) 876. doi: <https://doi.org/10.1016/j.catcom.2010.02.020>
- Wilson, K., Clark, J. H., Solid acids and their use as environmentally friendly catalysts in organic synthesis, *Pure Appl. Chem.* **72** (2000) 1313. doi: <https://doi.org/10.1351/pac200072071313>
- Choudhary, Vr., Jana, S. K., Benzylation of benzene and substituted benzenes by benzyl chloride over InCl₃, GaCl₃, FeCl₃, and ZnCl₂ supported on clays and Si-MCM-41, *J. Mol. Catal. A: Chem.* **180** (2002) 267. doi: [https://doi.org/10.1016/S1381-1169\(01\)00447-2](https://doi.org/10.1016/S1381-1169(01)00447-2)
- Vinu, A., Sawant, D. P., Ariga, K., Benzylation of benzene and other aromatics by benzyl chloride over mesoporous AISBA-15 catalysts, *Microporous Mesoporous Mater.* **80** (2005) 195. doi: <https://doi.org/10.1016/j.micromeso.2004.12.012>
- Xie, Y., Zhao, S., First principles study of Al and Ni segregation to the α -Fe/Cu (100) coherent interface and their effects on the interfacial cohesion, *Comput. Mater. Sci.* **63** (2012) 329. doi: <https://doi.org/10.1016/j.commatsci.2012.06.036>
- Stanislaus, A., Al, D. K., Absi, H. M., Preparation of a large pore alumina-based HDM catalyst by hydrothermal treatment and studies on pore enlargement mechanism, *J. Mol. Catal. A: Chem.* **181** (2002) 33. doi: [https://doi.org/10.1016/S1381-1169\(01\)00353-3](https://doi.org/10.1016/S1381-1169(01)00353-3)
- Shah, P., Ramaswamy, A. V., Ramaswamy, V., Lazar, K., Synthesis and characterization of tin oxide-modified mesoporous SBA-15 molecular sieves and catalytic activity in trans-esterification reaction, *Yingyong Huagong* **273** (2004) 239. doi: <https://doi.org/10.1016/j.apcata.2004.06.039>

24. Lu, L. B., Zu, Y., Wei, W. W., Liu, F., Cao, W., Jin, H., Chen, Y. N., Guo, L. J., Desulfurization mechanism of thiophene compounds in supercritical water, *Fuel* **353** (2023) 129251. doi: <https://doi.org/10.1016/J.FUEL.2023.129251>
25. Liu, Y., Deng, Q., Yao, Z., Liang, T., Zhang, S., Zhu, T., Xing, C., Pan, J., Yu, Z., Liang, K., Xie, T., Li, R., Hou, Y., Inducing spin polarization via Co doping in the BiVO₄ cell to enhance the built-in electric field for promotion of photocatalytic CO₂ reduction, *J. Colloid Interface Sci.* **664** (2024) 500. doi: <https://doi.org/10.1016/j.jcis.2024.03.078>
26. Hu, Y. M., Wang, P. X., Fu, L. Y., Yuan, Y., Wu, C. Y., Study on the effect of different preparation methods on ozone catalytic oxidation of aluminum-based catalysts, *Huanjing Kexue Yanjiu* **35** (2022) 2559. doi: <https://doi.org/10.13198/j.issn.1001-6929.2022.07.01>
27. Xue, Y., Chen, Z., Wu, Z., Tian, F., Yu, B., Hierarchical construction of a new Z-scheme Bi/BiVO₄-CdS heterojunction for enhanced visible-light photocatalytic degradation of tetracycline hydrochloride, *Sep. Purif. Technol.* **275** (2021) 119152. doi: <https://doi.org/10.1016/j.seppur.2021.119152>
28. Dasireddy, V. D. B. C., Likoar, B., Selective photocatalytic oxidation of benzene to phenol using carbon nanotube (CNT)-supported Cu and TiO₂ heterogeneous catalysts, *J. Taiwan Inst. Chem. Eng.* **82** (2018) 331. doi: <https://doi.org/10.1016/j.jtice.2017.11.011>
29. Wang, H., Zhao, W., Rehman, M. U., Copper phyllosilicate nanotube catalysts for the chemosynthesis of cyclohexane via hydrodeoxygenation of phenol, *ACS Catalysis* **12** (2022) 4724. doi: <https://doi.org/10.1021/acscatal.2c00380>
30. Tahir, M., Amin, N. S., Photocatalytic reduction of carbon dioxide with water vapors over montmorillonite modified TiO₂ nanocomposites, *Appl. Catal. B.* **142** (2013) 512. doi: <https://doi.org/10.1016/j.apcatb.2013.05.054>
31. Zhang, Z. Q., Peh, S. B., Wang, Y. X., Kang, C. J., Fan, W. D., Zhao, D., Efficient trapping of trace acetylene from ethylene in an ultramicroporous metal-organic framework: Synergistic effect of high-density open metal and electro-negative sites, *Angew. Chem.* **132** (2020) 19089. doi: <https://doi.org/10.1002/ange.202009446>
32. Qu, Q. H., Cheng, L. Y., Wang, P. R., Fang, C., Li, H. P., Ding, J., Wan, H., Guan, G. F., Guanidine-functionalized basic binuclear poly(ionic liquids) for low partial pressure CO₂ fixation into cyclic carbonate, *Sep. Tech.* **339** (2024) 126682. doi: <https://doi.org/10.1016/j.seppur.2024.126682>
33. Jiao, W. Z., Wei, X. Y., Shao, S. J., Liu, Y. Z., Catalytic decomposition and mass transfer of aqueous ozone promoted by Fe-Mn-Cu/ γ -Al₂O₃ in a rotating packed bed, *Chin. J. Chem. Eng.* **45** (2022) 133. doi: <https://doi.org/10.1016/J.CJCHE.2021.03.050>
34. Lv, F., He, L., Bai, X., Wang, D., Zhao, Y., Enhancing photocatalytic CO₂ reduction activity through Cobalt-Bismuth bimetallic nanoparticle-modified nitrogen-doped graphite carbon, *J. Colloid Interface Sci.* **675** (2024) 1069. doi: <https://doi.org/10.1016/j.jcis.2024.07.092>
35. Yue, Y. Y., Fu, J., Wang, C. M., Yuan, P., Bao, X. J., Xie, Z. L., Basset, J. M., Zhu, H. B., Propane dehydrogenation catalyzed by single Lewis acid site in Sn-Beta zeolite, *J. Catal.* **395** (2021) 155. doi: <https://doi.org/10.1016/J.JCAT.2020.12.019>
36. Shaikh, R. R., Damruang, S., Khan, R. A., Prasertdam, S., Prasertdam, P., Understanding the catalytic performance and deactivation behaviour of second-promoter doped Pt/WOx/ γ -Al₂O₃ catalysts in the glycerol hydrogenolysis for selective and cleaner production of 1,3-propanediol, *J. Energy Chem.* **94** (2024) 486. doi: <https://doi.org/10.1016/J.JECHEM.2024.02.067>
37. Prinetto, F., Ghiotti, G., Graffin, P., Didier, T., Synthesis and characterization of sol-gel Mg/Al and Ni/Al layered double hydroxides and comparison with co-precipitated samples, *Microporous Mesoporous Mater.* **39** (2000) 229. doi: [https://doi.org/10.1016/S1387-1811\(00\)00197-9](https://doi.org/10.1016/S1387-1811(00)00197-9)
38. Ren, Z. J., Jia, B., Zhang, G. M., Fu, X. L., Wang, Z. X., Wang, P. F., Lv, L. Y., Study on adsorption of ammonia nitrogen by iron-loaded activated carbon from low temperature wastewater, *Chemosphere* **26** (2021) 127895. doi: <https://doi.org/10.1016/j.chemosphere.2020.127895>
39. Sacco, N. A., Lovato, M. E., Marchesini, F. A., Devard, A. V., Synthesis design of Cu/Al₂O₃ catalysts to decrease copper leaching in the catalytic wet peroxide oxidation of phenol, *JHM Letters* **3** (2022) 100059. doi: <https://doi.org/10.1016/j.hazl.2022.100059>
40. Liu, T., Shi, L., Wang, Z. M., Liu, D. M., Preparation of Ag₂O/Bi₂O₃/Cl₂ p-n junction photocatalyst and its photocatalytic performance under visible and infrared light, *J. Liaoning Shiyou Huagong Daxue Xuebao* **632** (2022) 127811. doi: <https://doi.org/10.1016/j.colsurfa.2021.127811>
41. Hadi, P., Yeung, K. Y., Barford, J., Jin An, K., McKay, G., Significance of “effective” surface area of activated carbons on elucidating the adsorption mechanism of large dye molecules, *J. Environ. Chem. Eng.* **3** (2015) 1029. doi: <https://doi.org/10.1016/j.jece.2015.03.005>
42. Pinto, D., Minorello, S., Zhou, Z. P., Urakawa, A., Integrated CO₂ capture and reduction catalysis: Role of γ -Al₂O₃ support, unique state of potassium and synergy with copper, *Huanjing Kexue* **140** (2024) 113. doi: <https://doi.org/10.1016/j.jes.2023.06.006>
43. Wang, Q. Y., Zhang, H. H., Zhang, Y. L., Effect of roasting time on degradation of landfill leachate by Fe-Co-Ru-Ce/ γ -Al₂O₃ catalytic wet oxidation system, *SAMSE* (2019). doi: <https://doi.org/10.26914/c.cnkihy.2019.055461>
44. Sun, J. Y., Han, Y. X., Fu, H. Y., Wan, H. Q., Xu, Z. Y., Zheng, S. R., Selective hydrodechlorination of 1,2-dichloroethane catalyzed by trace Pd decorated Ag/Al₂O₃ catalysts prepared by galvanic replacement, *Sur. Sci.* **428** (2018) 703. doi: <https://doi.org/10.1016/j.apsusc.2017.09.168>
45. Li, Y., Xu, B., Yang, H., Jin, L. J., Hu, H. Q., Promotion of Cu/Ce supported red mud for NO removal from low and medium temperature flue gas, *Fuel Chem. Tech.* **52** (2024) 362. doi: [https://doi.org/10.1016/S1872-5813\(23\)60388-3](https://doi.org/10.1016/S1872-5813(23)60388-3)
46. Xiang, X. F., Zhang, B., Zhang, X. Y., Lu, X., Xu, H. J., Study on CO oxidation performance of Ce-Cu/ γ -Al₂O₃ catalyst in flue gas, *Reli. Fadian.* **50** (2021) 124. doi: <https://doi.org/10.19666/j.rlf.202012303>
47. Venkata, M. M. S., Bharath, P., Ramanjaneyulu, E., Ramachandran, D., Effect of roasting temperature on the structural, morphological, and magnetic properties of rare-earth orthoferrite NdFeO₃ nanoparticles synthesized by the sol-gel method, *ECS J. Solid State Sci. Technol.* **13** (2024) 083007. doi: <https://doi.org/10.1149/2162-8777/AD6D8B>
48. Javad, H. B., Amin, B., Mehran, R., Ehsan, A., Amirhosein, R. N., Elevating catalyst performance: How hierarchical alumina's phases enhance Cu/Al₂O₃ in reverse water-gas shift (RWGS) reaction, *Inter. Jour. Hydr. Ener.* **83** (2024) 717. doi: <https://doi.org/10.1016/j.ijhydene.2024.08.061>

49. *Chaube, V.*, Benzylolation of benzene to diphenylmethane using zeolite catalysts, *Catal. Commun.* **5** (2004) 321. doi: <https://doi.org/10.1016/j.catcom.2004.02.013>
50. *Chang, B., Wu, Y.*, Research on synthesis of diphenylmethane catalyzed by bisimidazolium ionic liquids, *Guangdong Huagong* **45** (2018) 26. doi: <https://doi.org/10.1016/j.issn.1011-1025.2018.12.14>
51. *Katabathini, N., Mohamed, M., Ebtesam, M. A.*, MoOx and WOx conjugated iron phosphate nanotubes catalysts for benzylolation of benzene using benzyl alcohol, *Catal. Commun.* **38** (2022) 106423. doi: <https://doi.org/10.1016/J.CATCOM.2022.106423>
52. *Zhao, Z. J., Wang, L., Zhang, X. D., Ding, W.*, Synthesis of diphenylmethane from benzene chlorination catalyzed by Fe-ZSM-5-SBA-15, *Yunnan Huagong* **48** (2021) 38. doi: <https://doi.org/10.3969/j.issn.1004-275X.2021.03.12>
53. *Xie, H. Y., Huang, C. Y., Yang, Z. Y., Wen, J. C., Wang, H., Xu, J. Q.*, Study on synthesis of diphenylmethane catalytic by Fe modified multi-level hole ZSM-5, *Jingxi Shiyong Huagong* **41** (2024) 9. doi: <https://doi.org/10.20075/j.cnki.issn.1003-9384.2024.03.003>
54. *Ning, L. M., Ling, J. H., Liu, D. M., Han, J. B., Wang, K.*, Research on the preparation of Cu-Al-MCM-41 and its catalytic synthesis of diphenylmethane, *Xiandai Huagong* **44** (2024) 116. doi: <https://doi.org/10.16606/j.cnki.issn0253-4320.2024.12.022>
55. *Zhang, Z. K., Xu, L. Y., Wang, Z. L., Xu, Y. J., Chen, Y. F.*, Pd/H β -zeolite catalysts for catalytic combustion of toluene: Effect of SiO₂/Al₂O₃ ratio, *Ziran Huaxue* **19** (2010) 417. doi: [https://doi.org/10.1016/S1003-9953\(09\)60091-8](https://doi.org/10.1016/S1003-9953(09)60091-8)
56. *Xuan, L. W., Wang, H., Zhang, J. Q., Wang, H. Y.*, Preparation of macroporous γ -Al₂O₃ and dehydrogenation of n-dodecane, *Dangdai Huagong* **41** (2012) 1030. doi: <https://doi.org/10.13840/j.cnki.cn21-1457/tq.2012.10.025>
57. *Sing, W. S. K.*, Reporting physisorption data for gas/solid systems with special reference to the determination of surface area and porosity (Provisional), *Pure Appl. Chem.* **54** (2013) 2201. doi: <https://doi.org/10.1351/pac198254112201>
58. *Li, Y. F., Su, J. J., Yu, F., Yan, X. L., Pan, D. H., Li, R. F., Yang, Y. X.*, Dehydrogenation of ethylbenzene with CO₂ over porous Co/Al₂O₃-ZrO₂ catalyst, *Cailiao Huaxue Wuli* **257** (2021) 123773. doi: <https://doi.org/10.1016/j.matchemphys.2020.123773>
59. *Tsai, L. H., Hseh, T. L., Chuin, T. Y., Shiann, H. C., Fong, C. S., Li, J. L., Chien, I. W.*, Electron microscopic studies on pore structure of alumina, *Appl. Catal. A* **158** (1997) 257. doi: [https://doi.org/10.1016/S0926-860X\(97\)00002-1](https://doi.org/10.1016/S0926-860X(97)00002-1)
60. *Li, N., Ding, J. J., Zhao, X. G., Zhao, H., Xu, Y. H.*, Preparation and catalytic properties of Fe₂O₃/ γ -Al₂O₃ in microwave-catalyzed reaction, *Huanjing Wuran Yu Fangzhi* **34** (2012) 9. doi: <https://doi.org/10.15985/j.cnki.1001-3865.2012.12.009>
61. *Serna, C. J., White, J. L., Hem, S. L.*, Structural survey of carbonate-containing antacids, *J. Pharm. Sci.* **67** (1978) 324. doi: <https://doi.org/10.1002/jps.2600670312>
62. *Sashkina, K. A., Rudina, N. A., Lysikov, A. I.*, Hierarchically porous materials built of Fe-silicalite nanobeads, *J. Mater. Chem. A* **2** (2014) 16061. doi: <https://doi.org/10.1039/C4TA02904F>
63. *Krruk, M., Jaronice, M.*, Gas adsorption characterization of ordered organic-inorganic nanocomposite materials, *Chem. Mater.* **13** (2001) 3169. doi: <https://doi.org/10.1021/cm0101069>
64. *He, P., Jarvis, J., Liu, L., Song, H.*, The promoting effect of Pt on the co-aromatization of pentane with methane and propane over Zn-Pt/HZSM-5, *Fuel* **239** (2019) 946. doi: <https://doi.org/10.1016/j.fuel.2018.11.079>
65. *Wang, W. Y., Yang, Y. Q., Luo, H.*, Ultrasound-assisted preparation of titania-alumina support with high surface area and large pore diameter by modified precipitation method, *J. Alloys Compd.* **509** (2011) 3430. doi: <https://doi.org/10.1016/j.jallcom.2010.12.119>
66. *Alaburdaitė, R., Krylova, V.*, Polypropylene film surface modification for improving its hydrophilicity for innovative applications, *Polym. Degrad. Stab.* **211** (2023) 110334. doi: <https://doi.org/10.1016/J.POLYMDEGRADSTAB.2023.110334>
67. *Chen, S., Zhang, Z., Wang, F. J., Xie, H. M., Jiao, Z. J., Zhou, G. L.*, Solvent assisted to prepare shell structured Cu/ γ -Al₂O₃ catalyst with low Cu content for oil efficient hydrodeoxygenation to high-quality biofuel, *Fuel* **357** (2024) 129870. doi: <https://doi.org/10.1016/j.fuel.2023.129870>
68. *He, H., Yang, C. X., Ouyang, J., Yang, Y. Q., Wang, F.*, Preparation and dehydrogenation of Ni-Cu/ γ -Al₂O₃ catalyst, *Jingxi Huagong* **28** (02011) 675. doi: <https://doi.org/10.13550/j.jxhg.2011.07.018>
69. *Candu, N., Florea, M., Coman, S., Parvulescu, V. I.*, Benzylolation of benzene with benzyl alcohol on zeolite catalysts, *Appl. Catal. A* **393** (2010) 206. doi: <https://doi.org/10.1016/j.apcata.2010.11.044>
70. *Fang, S. N., Jiang, M., Fu, Y. L., Lin, P. Y., Qiao, S., Xie, Y. N.*, Effect of calcination temperature on copper species structure of Cu/ γ -Al₂O₃ catalyst, *Wuli Huaxue Xuebao* **7** (1994) 623. doi: <https://doi.org/10.3866/PKU.WHXB19940709>
71. *Hentit, H., Bachari, K., Ouali, M., Womes, M., Benaichouba, B., Jumas, J. C.*, Alkylation of benzene and other aromatics by benzyl chloride over iron-containing aluminophosphate molecular sieves, *J. Mol. Catal. A: Chem.* **275** (2007) 158. doi: <https://doi.org/10.1016/j.molcata.2007.05.032>
72. *Ning, L. M., Han, J. B., Geng, Z. X., Liu, D. M., Fan, H. T., Bai, G. Y., Huang, Z. D.*, Cu-Al-MCM-41 catalysts for the selective synthesis of diphenylmethane: Influence of catalyst structure on activity and selectivity, *ChemistrySelect* **10** (2025) e202404552. doi: <https://doi.org/10.1002/slct.202404552>